JPEDAV (2007) 28:517–522
DOI: 10.1007/s11669-007-9202-y
1547-7037 ©ASM International

A Pseudoternary Phase Diagram of the BaO-ZrO_2-$ScO_{1.5}$ System at 1600 °C and Solubility of Scandia into Barium Zirconate

Susumu Imashuku, Tetsuya Uda, Tetsu Ichitsubo, Eiichiro Matsubara, and Yasuhiro Awakura

(Submitted October 19, 2006; in revised form January 17, 2007)

A pseudoternary phase diagram of the BaO-ZrO_2-$ScO_{1.5}$ system was established at 1600 °C, and solubility of scandia into barium zirconate was determined. According to the phase diagram, the solubility of scandia into barium zirconate at 1600 °C is 0.29 in a mole fraction of scandia ($X_{ScO_{1.5}}$) on the composition line where the mole fraction of barium oxide is 0.50. However, the solubility of scandia into barium zirconate is reduced with decreasing temperature and lies in between $X_{ScO_{1.5}}$ = 0.10 and 0.20 at 1300 °C.

Keywords phase diagram, pseudoternary, solubility limit

1. Introduction

The crystallographic structure of barium zirconate ($BaZrO_3$) is isomorphous with perovskite, and trivalent cation (M(III)) doped barium zirconate has been reported to be a proton conductive oxide.[1] It has great potential for applications, for example, electrolytes for fuel cells, hydrogen separation membrane, and hydrogen sensors. A trivalent cation in a Zr(IV) site forms an oxide ion vacancy in the structure as given in Eq 1:

$$2Zr_{Zr}^{x} + O_{O}^{x} + M_2O_3 \rightarrow 2M'_{Zr} + V_{O}^{\bullet\bullet} + 2ZrO_2 \qquad \text{(Eq 1)}$$

where Kröger-Vink notation is adopted. A water molecule from the gas phase dissociates into a hydroxide ion and a proton in the oxides; the hydroxide ion fills an oxide ion vacancy, and the proton forms a hydroxide ion with lattice oxygen. This proton shows protonic conduction by jumping to the vicinity of an oxygen site and rotating around the oxygen.

The solubility of the dopant is quite important information for evaluating the protonic conductivity. Currently, we are focusing on scandium-doped barium zirconate because the ionic radius of scandium is almost the same as that of zirconium (Zr^{4+}: 0.072 nm, Sc^{3+}: 0.0745 nm for six-fold coordination[2]). It is expected that the solubility of scandia (Sc_2O_3) into barium zirconate will be higher than that of any other trivalent cations. In fact, Omata et al. reported a dopant-clustering phenomenon in yttrium-doped barium zirconate (the ionic radius of yttrium is 0.0900 nm for six-fold coordination[2]) by IR spectroscopy, but they did not observe such a phenomenon in scandium-doped barium zirconate.[3] In addition, the phase separation of barium zirconate phase in yttrium-doped barium zirconate was reported.[4] Therefore, we intended to establish a pseudoternary phase diagram of the BaO-ZrO_2-$ScO_{1.5}$ system at 1600 °C, which is a typical sintering temperature of barium zirconate, and investigate the solubility of scandia into barium zirconate at 1300 and 1600 °C.

Susumu Imashuku, Tetsuya Uda, Tetsu Ichitsubo, Eiichiro Matsubara, and **Yasuhiro Awakura,** Department of Materials Science and Engineering, Kyoto University, Yoshida-Hommachi, Kyoto 606-8501, Japan. Contact e-mail: s.imashuku@t25y0243.mbox.media.kyoto-u.ac.jp.

2. Experimental

2.1 Chemical Analysis and Phase Identification

The nominal compositions of samples examined in this work are listed in Table 1 with results of phase identification by x-ray diffraction analysis (XRD; RINT2200, Cu Kα, Rigaku Corporation, Tokyo, Japan). Figure 1 shows the nominal compositions of prepared samples on a pseudoternary phase diagram of the BaO-ZrO_2-$ScO_{1.5}$ system. Average compositions of samples and the compositions of each grain in samples were analyzed by energy-dispersive x-ray microanalysis (EDX) (JED-2300, JEOL, Tokyo, Japan) equipped with field emission scanning electron microscope (FE-SEM) (JSM-6500F, JEOL, Tokyo, Japan). The compositions of each grain in samples by EDX were calibrated based on the assumption that the average compositions of samples analyzed by EDX are equal to the nominal compositions. Some results of average composition were reproduced by inductively coupled plasma atomic emission spectroscopy (ICP-AES) (SPS4000, Seiko Instruments Inc., Chiba, Japan) within the error of the instrument.

2.2 Material Preparation

All samples were synthesized by a solid-state reaction from barium carbonate ($BaCO_3$: 99.9%, Wako), zirconia

Table 1 Nominal compositions of samples and phases identified by x-ray diffraction in samples heat treatment at 1600 °C for 24 h in air

	Nominal composition			Identified phase by XRD			
Sample	X_{BaO}	X_{ZrO_2}	$X_{ScO_{1.5}}$	$BaZrO_3$(ss)	ZrO_2 (cubic)	$ScO_{1.5}$	$Ba_3Sc_4O_9$(ss)
A	0.300	0.650	0.050	Detected	Detected	Undetected	Undetected
B	0.300	0.550	0.150	Detected	Detected	Undetected	Undetected
C	0.300	0.450	0.250	Detected	Detected	Detected	Undetected
D	0.300	0.350	0.350	Detected	Detected	Detected	Undetected
E	0.300	0.250	0.450	Detected	Undetected	Detected	Undetected
F	0.300	0.150	0.550	Detected	Undetected	Detected	Undetected
G	0.300	0.050	0.650	Detected	Undetected	Detected	Undetected
H	0.500	0.500	0	Detected	Undetected	Undetected	Undetected
I	0.500	0.400	0.100	Detected	Undetected	Undetected	Undetected
J	0.500	0.300	0.200	Detected	Undetected	Undetected	Undetected
K	0.500	0.250	0.250	Detected	Undetected	Undetected	Undetected
L	0.500	0.200	0.300	Detected	Undetected	Undetected	Detected

ss means solid solution

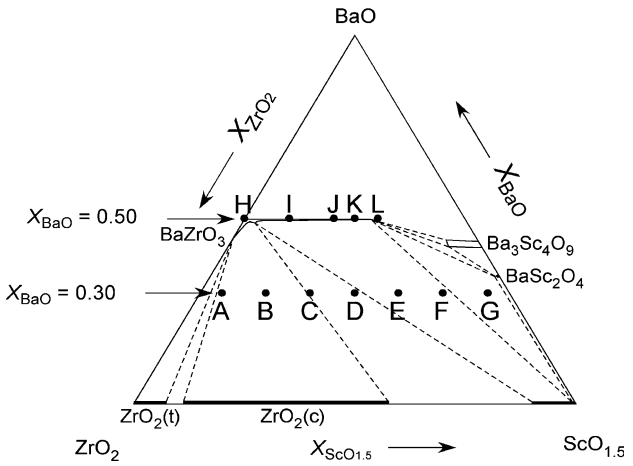

Fig. 1 Nominal compositions of samples used in this study at 1600 °C for 24 h. Abbreviations of sample names are referred to in Table 1

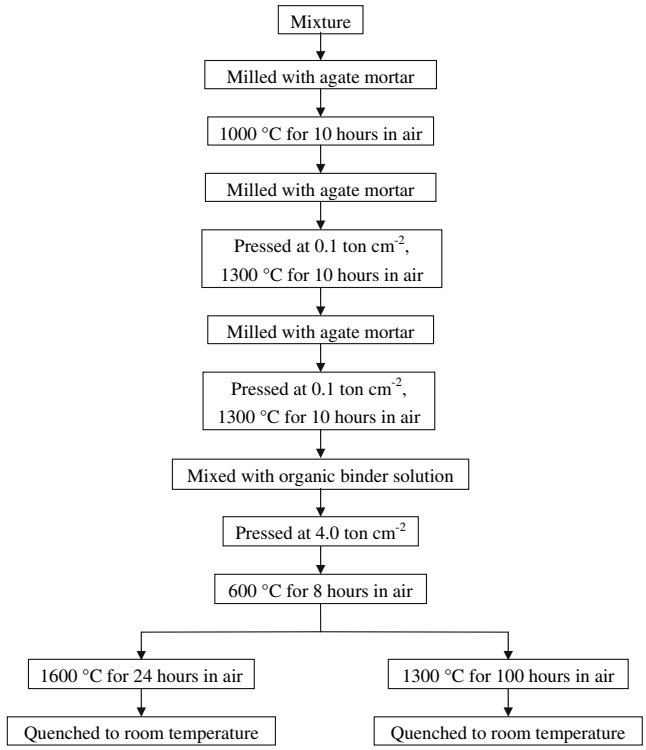

Fig. 2 Synthesis procedures of samples. Abbreviations of sample names are referred to in Table 1

(ZrO_2: 99.97% including 1.5 to ~2 mass% of hafnia (HfO_2), Daiichi Kigenso) and scandia (99.9%, Pacific Metals). The chemical properties of hafnium are quite similar to those of zirconium. Thus, hafnium is expected to substitutionally replace zirconium in proportion to its atomic percentage. In addition, 1.5 mass% of hafnia corresponds to only 0.9 mol% of hafnia in the ZrO_2-HfO_2 system. Such a small percentage does not affect the composition analysis beyond the error of the instruments. Thus, the authors neglected the effect of hafnia on the results. Flow charts of synthesis procedures of samples are shown in Fig. 2. All samples were finally calcined at 1300 °C in air and pressed into pellets. The samples were heat treated at 1300 °C for 100 h or 1600 °C for 24 h in air. Heated samples were quenched to room temperature. At elevated temperatures, barium oxide (BaO) has a significant vapor pressure ($\sim 8\times10^{-5}$ atm at 1600 °C[5]). There is a possibility for a part of the barium oxide in the samples to vaporize, which causes deviation of the sample composition from the nominal compositions. Therefore, a powder bed of 90 mass% of scandium-doped barium zirconate and 10 mass% of barium carbonate was

used to suppress the vaporization of barium oxide when mole fraction of barium oxide is 0.50 (X_{BaO} = 0.50).

3. Results and Discussion

We established the pseudoternary phase diagram of the BaO-ZrO_2-$ScO_{1.5}$ system at 1600 °C as shown in Fig. 3. To establish this phase diagram, we combined information of pseudobinary phase diagrams of a BaO-ZrO_2 system[6] and a BaO-$ScO_{1.5}$ system,[7] and the solubility of scandia into tetragonal and cubic zirconia phase.[8] There is only one reported phase diagram for the BaO-ZrO_2 system and BaO-$ScO_{1.5}$ system. On the other hand, there are many proposed phase diagrams for a ZrO_2-$ScO_{1.5}$ system.[8-14] Among these phase diagrams, the phase relationship at 1600 °C coincides well, and the solubility of scandia into tetragonal and cubic

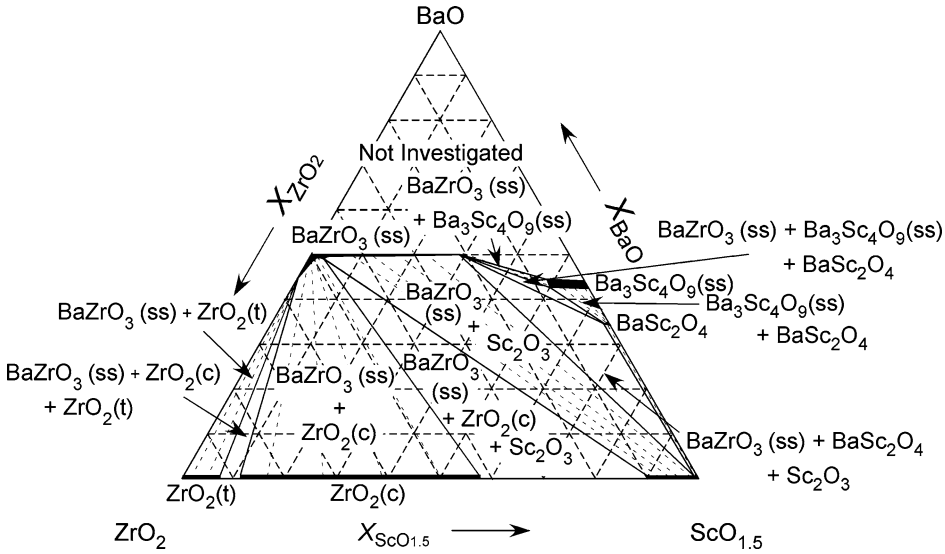

Fig. 3 Established pseudoternary phase diagram of the BaO-ZrO_2-$ScO_{1.5}$ system at 1600 °C. ZrO_2(t) and ZrO_2(c) denote tetragonal zirconia and cubic zirconia, respectively

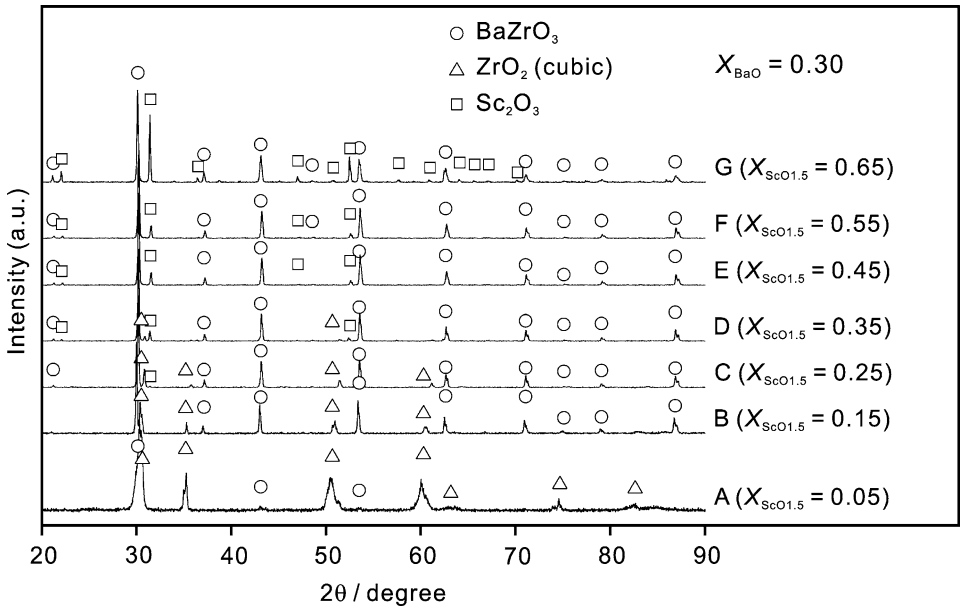

Fig. 4 XRD patterns of samples of $X_{ScO_{1.5}}$ = 0.05, 0.15, 0.25, 0.35, 0.45, 0.55, and 0.65 at X_{BaO} = 0.30 after heat treating at 1600 °C for 24 h

Table 2 Compositions of each phase in samples on the composition line of X_{BaO} = 0.30

		$BaZrO_3$(ss)			ZrO_2			Sc_2O_3			$BaSc_2O_4$		
	$X_{ScO_{1.5}}$	X_{BaO}	X_{ZrO_2}	$X_{ScO_{1.5}}$	X_{BaO}	X_{ZrO_2}	$X_{ScO_{1.5}}$	X_{BaO}	X_{ZrO_2}	$X_{ScO_{1.5}}$	X_{BaO}	X_{ZrO_2}	$X_{ScO_{1.5}}$
A	0.05	0.45	0.54	0.00	0.00	0.86	0.14	n.d.	n.d.	n.d	n.d.	n.d.	n.d.
B	0.15	0.48	0.51	0.01	0.00	0.59	0.41	n.d	n.d.	n.d	n.d.	n.d.	n.d.
C	0.25	0.50	0.49	0.01	0.00	0.41	0.59	0.00	0.10	0.89	n.d.	n.d.	n.d.
D	0.35	0.49	0.48	0.03	0.00	0.48	0.51	0.00	0.10	0.90	n.d.	n.d.	n.d.
E	0.45	0.50	0.40	0.11	n.d.	n.d.	n.d.	0.01	0.01	0.98	n.d.	n.d.	n.d.
F	0.55	0.50	0.28	0.22	n.d.	n.d.	n.d.	0.00	0.01	0.99	n.d.	n.d.	n.d.
G	0.65	0.50	0.20	0.29	n.d.	n.d.	n.d.	0.01	0.00	0.99	0.35	0.01	0.63

ss means solid solution
n.d. means not detected

zirconia phase at 1600 °C is almost the same.[8,10-12,14] We adopted the values from the newest phase diagram of the ZrO_2-$ScO_{1.5}$ system reported by Yashima et al.[8]

3.1 Analysis of X-Ray Diffraction of Samples of X_{BaO} = 0.30

Samples on the composition line of X_{BaO} = 0.30 were heat treated at 1600 °C for 24 h. X-ray diffraction patterns of the samples are shown in Fig. 4, and the identified phases are summarized in Table 1. When the mole fraction of scandia was 0.05 [$X_{ScO_{1.5}}$ = 0.05 (sample A)] and 0.15 [$X_{ScO_{1.5}}$ = 0.15 (sample B)], barium zirconate phase and cubic zirconia phase were identified. When $X_{ScO_{1.5}}$ = 0.25 (sample C) and 0.35 (sample D), barium zirconate phase, scandia phase, and cubic zirconia phase were identified. As seen in Fig. 4, the peak positions of the cubic zirconia phase in sample B ($X_{ScO_{1.5}}$ = 0.15), sample C ($X_{ScO_{1.5}}$ = 0.25), and sample D ($X_{ScO_{1.5}}$ = 0.35) shifted to higher angles than those of the cubic zirconia phase in JCPDS card (No. 270997, lattice parameter, a = 0.50900 nm), which is probably due to dissolution of scandia into the cubic zirconia phase. When $X_{ScO_{1.5}}$ = 0.45 (sample E), 0.55 (sample F), and 0.65 (sample G), barium zirconate phase and scandia phase were identified. The intensities of the peaks of the scandia phase increased with increasing mole fraction of scandia.

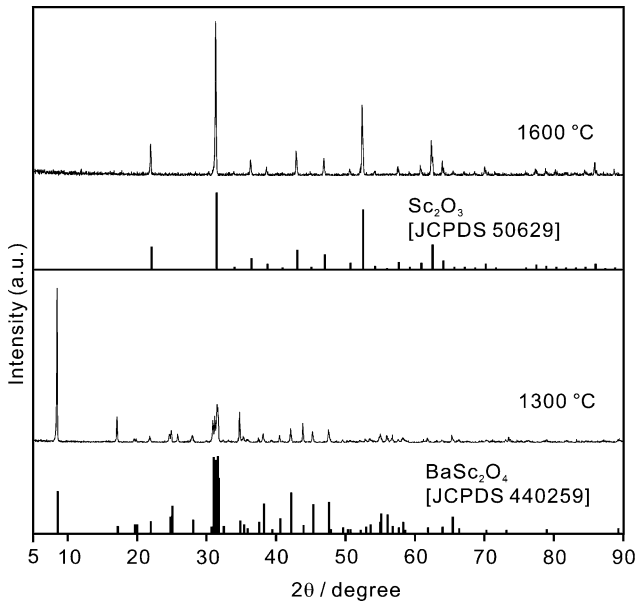

Fig. 5 XRD patterns of $BaSc_2O_4$ at 1300 and 1600 °C

3.2 Results of EDX Analysis of Samples of X_{BaO} = 0.30

Table 2 shows the compositions of each grain in the samples on the composition line of X_{BaO} = 0.30. Four types of grains were observed in this study. At $X_{ScO_{1.5}}$ = 0.65 (sample G), $BaSc_2O_4$ phase was observed by EDX analysis, although no diffraction pattern corresponding to $BaSc_2O_4$ phase was detected by XRD analysis. To investigate the reason, we synthesized a single phase of $BaSc_2O_4$ and heat treated at 1300 °C for 100 h or 1600 °C for 24 h, and then quenched to room temperature. Figure 5 shows XRD patterns of $BaSc_2O_4$ at 1300 and 1600 °C. The XRD pattern of $BaSc_2O_4$ phase at 1600 °C is completely different from that at 1300 °C, and the XRD pattern of $BaSc_2O_4$ phase at 1600 °C does not coincide with that in JCPDS

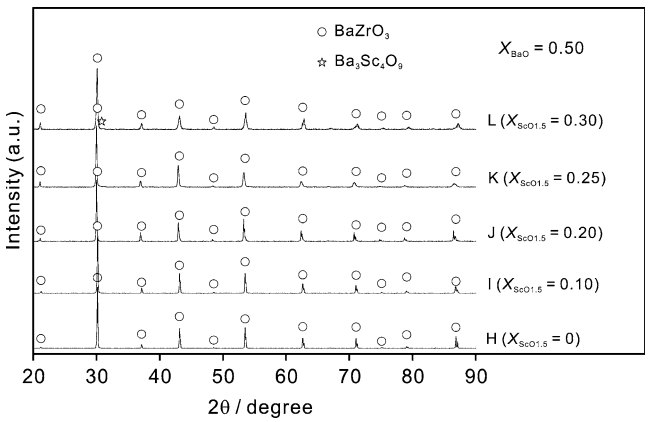

Fig. 6 XRD patterns of $X_{ScO_{1.5}}$ = 0, 0.10, 0.20, 0.25, and 0.30 at X_{BaO} = 0.50 after heat treating at 1600 °C for 24 h

Table 3 Phases identified by XRD in the samples on the composition line of X_{BaO} = 0.50 after heat treatment at 1300 and 1600 °C

XbaO	X_{ZrO_2}	$X_{ScO_{0.15}}$	1300 °C×100 h	1600 °C×24 h	As synthesized at 1300 °C
0.500	0.400	0	$BaZrO_3$	$BaZrO_3$	$BaZrO_3$
0.500	0.250	0.100	$BaZrO_3$(ss) + Sc_2O_3	$BaZrO_3$(ss)	$BaZrO_3$(ss)
0.500	0.300	0.200	$BaZrO_3$(ss) + $Ba_3Sc_4O_9$(ss)	$BaZrO_3$(ss)	$BaZrO_3$(ss) + $Ba_3Sc_4O_9$(ss)
0.500	0.250	0.250	$BaZrO_3$(ss) + $Ba_3Sc_4O_9$(ss) + Sc_2O_3	$BaZrO_3$(ss)	$BaZrO_3$(ss) + $Ba_3Sc_4O_9$(ss)
0.500	0.200	0.300	$BaZrO_3$(ss) + $Ba_3Sc_4O_9$(ss)	$BaZrO_3$(ss)	$BaZrO_3$(ss) + $Ba_3Sc_4O_9$(ss)

ss means solid solution

card (No. 440259, lattice parameter, a = 0.98341 nm, b = 0.58159 nm, c = 2.0578 nm). In contrast, the XRD pattern of $BaSc_2O_4$ phase at 1600 °C is quite similar to that of the scandia phase (JCPDS No. 50629, C-type rare earth structure). We are assuming that the high-temperature structure of $BaSc_2O_4$ is an isostructure with C-type rare earth structure, and there is a phase transition of $BaSc_2O_4$ between 1300 and 1600 °C.

3.3 Analysis of X-Ray Diffraction and Results of EDX Analysis of Samples of X_{BaO} = 0.50

Figure 6 shows XRD patterns of samples at X_{BaO} = 0.50 that were heat treated at 1600 °C for 24 h, and the identified phases are summarized in Table 1. When the mole fraction of scandia was from $X_{ScO_{1.5}}$ = 0 to 0.25 (sample H to K), only the barium zirconate phase was detected. By EDX analysis, it was confirmed that all grains of the barium zirconate phase in the samples from $X_{ScO_{1.5}}$ = 0 to 0.25 (sample H to K) had the same compositions as the average compositions of each sample. At $X_{ScO_{1.5}}$ = 0.30 (sample L), peak patterns of barium zirconate phase and $Ba_3Sc_4O_9$ phase were identified by XRD analysis. The mole fraction of scandia in the barium zirconate phase of the sample at $X_{ScO_{1.5}}$ = 0.30 (sample L) was 0.29 by EDX analysis. Thus, the solubility of scandia into barium zirconate at X_{BaO} = 0.50 is determined to be $X_{ScO_{1.5}}$ = 0.29 at 1600 °C. At $X_{ScO_{1.5}}$ = 0.30 (sample L), the peak positions of the $Ba_3Sc_4O_9$ phase shifted to lower angles than those of the $Ba_3Sc_4O_9$ phase in the JCPDS card (No. 310161, lattice parameter, a = 0.57989 nm, c = 2.3671 nm). Thus, it is assumed that $Ba_3Sc_4O_9$ has some solubility of zirconia.

3.4 Solubility of scandia into barium zirconate at 1300 °C

We examined the solubility of scandia into barium zirconate at temperatures lower than 1600 °C. Samples were heat treated at 1300 °C for 100 h in air. Table 3 shows the phases identified by XRD in samples on the composition line of X_{BaO} = 0.50.

Barium zirconate phase was only detected at $X_{ScO_{1.5}}$ = 0. Barium zirconate phase and scandia phase were identified when $X_{ScO_{1.5}}$ = 0.10. When heat treated at 1300 °C, samples were not covered with a powder bed of scandium-doped barium zirconate and barium carbonate. Thus, we assumed that a small part of the barium oxide vaporized from the surface of the sample and that the composition of the sample moved to a two-phase region of barium zirconate phase and scandia phase. In fact, the negative deviation from the average composition of barium oxide at $X_{ScO_{1.5}}$ = 0.10 was confirmed by ICP-AES (X_{BaO} = 0.488, X_{ZrO_2} = 0.423, and $X_{ScO_{1.5}}$ = 0.090). Thus, we assume that the solubility of scandia is more than $X_{ScO_{1.5}}$ = 0.10. When $X_{ScO_{1.5}}$ = 0.20 and 0.30, barium zirconate phase and $Ba_3Sc_4O_9$ phase were identified. When $X_{ScO_{1.5}}$ = 0.25, barium zirconate phase, scandia phase, and $Ba_3Sc_4O_9$ phase were identified. This might be due to the same reason as when $X_{ScO_{1.5}}$ = 0.10 and the composition at $X_{ScO_{1.5}}$ = 0.25 was X_{BaO} = 0.474, X_{ZrO_2} = 0.273, and $X_{ScO_{1.5}}$ = 0.253 by ICP-AES. $Ba_3Sc_4O_9$ phase was not detected at $X_{ScO_{1.5}}$ = 0.10. Therefore, the solubility of scandia into barium zirconate at X_{BaO} = 0.50 at 1300 °C is estimated to be between $X_{ScO_{1.5}}$ = 0.10 and $X_{ScO_{1.5}}$ = 0.20. In addition, the peak positions of the $Ba_3Sc_4O_9$ phase did not shift at all. Thus, we can assume that $Ba_3Sc_4O_9$ has very small solubility of zirconia at 1300 °C.

4. Conclusions

The results obtained in this work can be summarized:

- A part of the pseudoternary phase diagram in the BaO-ZrO_2-$ScO_{1.5}$ system at 1600 °C was established. According to the phase diagram, the solubility of scandia into barium zirconate is $X_{ScO_{1.5}}$ = 0.29 on the composition line where the mole fraction of barium oxide is 0.50 (X_{BaO} = 0.50). However, at 1300 °C, the solubility of scandia into barium zirconate is between $X_{ScO_{1.5}}$ = 0.10 and $X_{ScO_{1.5}}$ = 0.20.
- Zirconia can dissolve into $Ba_3Sc_4O_9$. However, $Ba_3Sc_4O_9$ does not have such solubility of zirconia at 1300 °C.
- $BaSc_2O_4$ has a phase transition between 1300 and 1600 °C.

Acknowledgments

This study was supported by Industrial Technology Research Grant Program in 2006 from New Energy and Industrial Technology Development Organization (NEDO) of Japan. We also express our deep acknowledgement to Daiichi Kigenso Kagaku Kogyo Co., Ltd and Pacific Metals

Co., Ltd for the supply of zirconia powder and scandia powder, respectively.

References

1. H. Iwahara, T. Yajima, T. Hibino, K. Ozaki, and H. Suzuki, Protonic Conduction in Calcium, Strontium, and Barium Zirconates, *Solid State Ionics*, 1976, **61**, p 65-69
2. R.D. Shannon, Revised Effective Ionic-radii and Systematic Studies of Interatmic Distances in Halides and Chalcogenides, *Acta Crystallogr., Sect. A: Cryst. Phys., Diffr., Theor. Gen. Crystallogr.*, 1976, **32**, p 751
3. T. Omata, Y. Noguchi, and S. Otuka-Yao-Matsuo, Infrared Study of High-Temperature Proton-Conducting Aliovalently Doped $SrZrO_3$ and $BaZrO_3$, *J. Electrochem. Soc.*, 2005, **152**, p 200-205
4. A. Kojima, K. Tanaka, Y. Oyama, T. Higuchi, and S. Yamaguchi, Phase equilibrium and thermodynamic stability in the BaO-ZrO2-$YO_{1.5}$ system, *The 31st Symposium on Solid State Ionics in Japan*, 2005, p 100-101
5. I. Barin, *Thermochemical Data of Pure Substances*, 3rd ed., VCH Verlagsgesellschaft mbH, 1995
6. J.O.A. Paschoal, H. Kleykamp, and F. Thümmler, Phase Equilibria in the Pseudoquaternary BaO-UO_2-ZrO_2-MoO_2 System, *J. Nucl. Mater.*, 1987, **151**, p 10-21
7. L.M. Kovba, L.N. Lykova, M.V. Paromova, and T.A Kalinina, X-ray Diffraction and Thermographic Studies of Compounds in the BaO-Sc_2O_3 System, *Dokl. Akad. Nauk SSSR*, 1981, **260**(4), p 924-927, (in Russian)
8. M. Yashima, M. Kakihana, and M. Yoshimura, Metastable-Stable Phase Diagrams in the Zirconia-Containing Systems Utilized in Solid-Oxide Fuel Cell Application, *Solid State Ionics*, 1996, **86-88**, p 1131-1149
9. F.M. Spiridonov, L.N. Popova, and R.Y.A. Popil'skii, On the Phase Relations and the Electrical Conductivity in the System ZrO_2-Sc_2O_3, *J. Solid State Chem.*, 1970, **2**, p 430-438
10. M.R. Thornber, D.J.M. Bevan, and E. Summerville, Mixed Oxides of the Type MO_2(Fluorite)-M_2O_3. V. Phase Studies in the Systems ZrO_2-M_2O_3 (M = Sc, Yb, Er, Dy), *J. Solid State Chem.*, 1970, **1**, p 545-553
11. R. Ruh, H.J. Garret, R.F. Domagala, and V.A. Patel, The System Zirconia-Scandia, *J. Am. Ceram. Soc.*, 1997, **60**(9-10), p 399-403
12. A.V. Shevchenko, I.M. Maister, and L.M. Lopato, Reactions in the HfO_2-Sc_2O_3 and ZrO_2-Sc_2O_3 Systems at High-Temperatures, *Inorg. Mater.*, 1987, **23**, p 1169-1173
13. R.L. Magunov, G.L. Shklyar, and V.F. Katridi, Phase-Diagram of the ZrO_2(HfO_2)-SC_2O_3 System, *Inorg. Mater.*, 1989, **25**, p 1035-1037
14. T.-S. Sheu, J. Xu, and T.-Y. Tien, Phase Relationship in the ZrO_2-Sc_2O_3 and ZrO_2-In_2O_3 Systems, *J. Am. Ceram. Soc.*, 1993, **76**(8), p 2027-2032